

Uncertainty Quantification for the Flow of Nanofluids in Converging/Diverging Channels

R. Gul¹, A. Shahzad¹, W. A. Khan², and W. Al-Kouz^{3,*}

¹Department of Mathematics, COMSATS University Islamabad, Abbottabad Campus, Pakistan

²Department of Mechanical Engineering, College of Engineering, Prince Mohammad Bin Fahd University, Al Khobar 31952, Kingdom of Saudi Arabia

³Mechatronics Engineering Department, German Jordanian University, Amman, Jordan

*corresponding author: wael.alkouz@gju.edu.jo

Abstract:

In mathematical models, parameters are one of the most important input factors that affect the model outputs. In this work, the effects of parameters in complement with their interactions effects on output variables of nanofluids in both converging and diverging channels has been studied. The mathematical model is solved numerically by using Matlab built-in solver bvp4c. Global sensitivity analysis (Sobol's method) is used to quantify the effects of input parameters and their interactions on model outputs. The results showed that the channel opening (α) is the most influential parameter for the velocity profile, while Eckert number (Ec) becomes the most influential parameter for temperature distribution in both diverging and converging channels. Also, the least sensitive parameters, as well as interaction effects of involved parameters are identified on velocity and temperature profiles in both converging and diverging channels.

Keywords: Uncertainty quantification; Sensitivity analysis; Sobol's method; Nanofluids; converging and diverging channels;

1. Introduction

In recent times, nanofluids have gained much importance due to many engineering and industrial applications. The use of nanofluids as coolants in industries, as drug transferring agent in biomedical engineering, as nanochips in electronic devices and war heads are some of the applications. The main idea of nanofluids can be traced back to Choi [1], who in a landmark study proposed the idea. Theoretically, nanofluid is a suspension of nanoparticles and a working fluid, where working fluid is termed as base fluid. The lack of heat transfer of typical fluids such as water, the kerosene oil, lubricants and the traditional coolants made the researchers to look for more

efficient heat transfer fluids. Further studies have proved that the use of nanofluids can increase the heat transfer capacity of traditional fluids upto 40% [2-4]. Also, researchers implemented the experimentally developed models for the analysis of heat and mass transfer in various situations. Like, for example flow over stretching surfaces [5,6], flow in channels [7,8], flow over wedge [9,10]. One of the studies that has gained interest is the flow through convergent and divergent channels, traditionally known as the Jeffery-Hamel flows [11,12]. Recently, Khan et al [13] studied the flow of nanofluids in converging and diverging channels. They used Cu-Water nanofluids for the analysis. In another related study, Khan et al [14] presented the flow and heat transfer in converging and diverging channels suspended by carbon nanotubes. Extending the same, Mohyud-Din et al [15] used the carbon nanotubes for analyzing the behavior of nanofluids in converging and diverging channels.

In this study, we analyzed and studied a new aspect i.e. how the behavior of nanofluids are effected by variations of involved parameters within a feasible regions? Which can be done using sensitivity analysis. Mainly, two approaches are common to conduct parametric sensitivity analysis i.e. local and global sensitivity analysis. In local sensitivity analysis (LSA), the value of one parameter at one time is changed around its base value to study the impact of that parameter on output variables [16,17]. The process is repeated for all parameters individually and their impacts are studied on outputs variables. The methods of LSA are also known as one-(parameter)-at-a-time (OAT), which are simple and computationally efficient. While, LSA techniques are not appropriate to study the impacts of feasible regions of input factors (here parameters) and their mutual effects on outputs variables. In such scenarios, GSA is more suitable approach to study the impacts of feasible regions of input parameters and their mutual effects on outputs variables [18-24]. Recently, Darbari et al. [25] employed the response surface technique in nanofluid and observed that entropy generation is more sensitive than Reynolds number. Further, Mackolil et al. [26] employed the same methodology and studied the sensitivity analysis in Casson nanofluids under heat absorption effects. They noticed that Nusselt number has a positive sensitivity toward thermal radiation. While, Fadodun et al [27], investigated the entropy production rate in $\text{Al}_2\text{O}_3/\text{H}_2\text{O}$ nanofluid using response surface methodology.

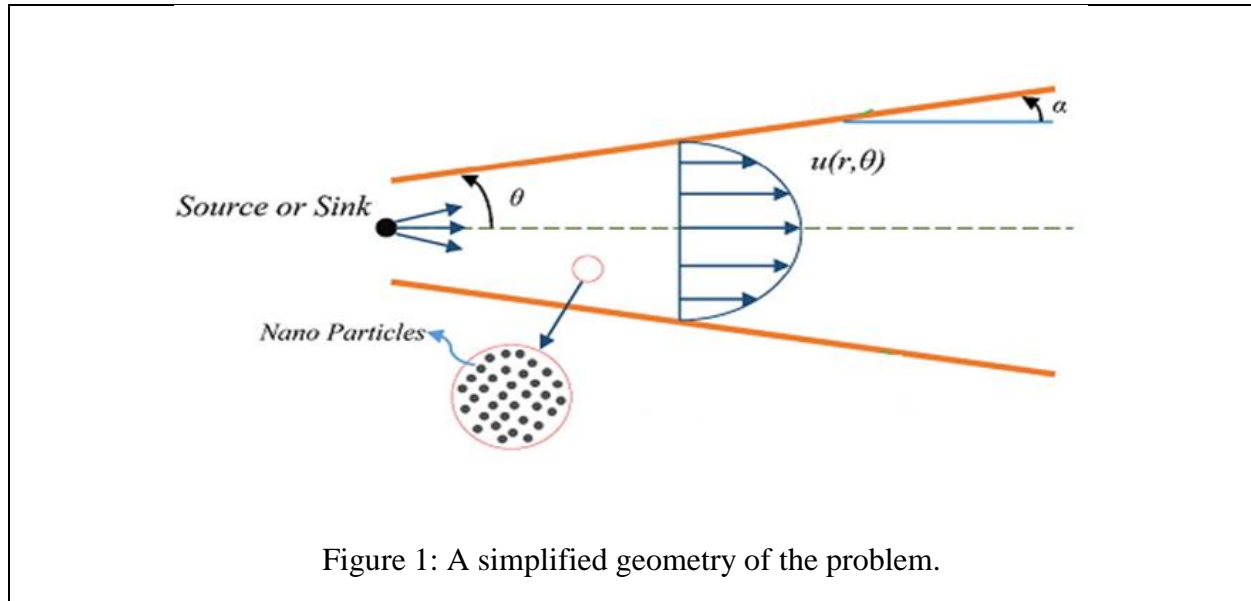
Motivated with the importance of sensitivity analysis, it is aim to identify the most important parameter that influence the flow of nanofluid in converging/diverging channels. Within this work, we applied the global sensitivity analysis; the method of Sobol to identify the ranking of key

parameters, factor fixing and mutual effects of parameters on the flow of nanofluid in converging diverging channels. Before applying the sensitivity analysis, it is very important to identify the input and output quantities of interest (QoI). In this paper, the input QoI are model parameters (α, Re, ϕ, Ec) and output QoI are velocity profile and temperature distribution of nanofluid under consideration. The objectives of this research work are summarised as:

- (i). Identify the most and least influential model parameters of nanofluid in convergent/ divergent channels.
- (ii). Ranking the most important model parameters and factor fixing
- (iii). Identify the mutual (interaction) effects of parameters on output QoI.

2. Mathematical model

Here, we consider an incompressible fluid flow, where flow is produced via source or a sink. The angle between the wall is 2α , see Figure (1). The flow is considered to be purely radial and symmetric of nature. The medium is filled with water (base fluid) and it contains copper Cu as the nanoparticles. Thermal equilibrium between water and copper is assumed with no slip at the walls of the channel, where the velocity field, $V = [u_r, 0, 0]$ with $u_r = u_r(r, \theta)$.



By considering the earlier mentioned assumptions, the polar form of continuity, momentum and the energy equations in absence of body forces are [14],

$$\frac{1}{r} \frac{\partial}{\partial r}(ru_r) = 0 \quad (1)$$

$$\rho_{nf} \left(u_r \frac{\partial u_r}{\partial r} \right) = -\frac{\partial P}{\partial r} + \mu_{nf} \left[\frac{\partial^2 u_r}{\partial r^2} + \frac{1}{r} \frac{\partial u_r}{\partial r} + \frac{1}{r^2} \frac{\partial^2 u_r}{\partial \theta^2} - \frac{u_r}{r^2} \right] \quad (2)$$

$$\frac{-1}{\rho_{nf} r} \frac{\partial P}{\partial r} + \frac{2}{r^2} \frac{\mu_{nf}}{\rho_{nf}} \frac{\partial u_r}{\partial \theta} = 0 \quad (3)$$

$$u_r \frac{\partial T}{\partial r} = \frac{k_{nf}}{(\rho C p)_{nf}} \left[\frac{\partial^2 T}{\partial r^2} + \frac{1}{r} \frac{\partial T}{\partial r} + \frac{1}{r^2} \frac{\partial^2 T}{\partial \theta^2} \right] + \mu_{nf} \left[4 \left(\frac{\partial u_r}{\partial r} \right)^2 + \frac{1}{r^2} \left(\frac{\partial u_r}{\partial \theta} \right)^2 \right] \quad (4)$$

Supporting boundary conditions are,

$$u_r = U, \quad \frac{\partial u_r}{\partial \theta} = 0, \quad \text{and} \quad \frac{\partial T}{\partial \theta} = 0 \quad \text{at} \quad \theta = 0$$

$$u_r = 0, \quad T = T_w \quad \text{at} \quad \theta = \alpha$$

where, T_w is the temperature at the wall.

The continuity equation given in (1), can be written as,

$$f(\theta) = ru_r(r, \theta) \quad (5)$$

The following expressions are being used for dimensionless form as,

$$f(\eta) = \frac{f(\theta)}{f_{\max}}, \quad \eta = \frac{\theta}{\alpha}, \quad \beta(\eta) = \frac{T}{T_w} \quad (6)$$

Elimination of pressure P from Eqs. (2), (3) and implementation of Eqs. (5) and (6) gives a nonlinear system of equations of the form;

$$F'''(\eta) + 2\alpha \text{Re}(1-\phi)^{2.5} A_1 F(\eta) F'(\eta) + 4\alpha^2 F'(\eta) = 0 \quad (7)$$

$$\beta''(\eta) + \frac{A_2 Ec \text{Pr}}{A_3 (1-\phi)^{2.5}} \left[4\alpha^2 F^2(\eta) + (F'(\eta))^2 \right] = 0 \quad (8)$$

With boundary conditions, using Eqs (5) and (6) are

$$F(0) = 1, \quad F'(0) = 1, \quad F(1) = 0, \quad \beta(1) = 1, \quad \text{and} \quad \beta'(0) = 0 \quad (9)$$

Where, Re denotes Reynolds number given by,

$$\text{Re} = \frac{f}{\nu} = \frac{Ur\alpha}{\nu} \begin{pmatrix} \text{Divergent-Channel} : \alpha > 0, U > 0 \\ \text{Convegent-Channel} : \alpha < 0, U < 0 \end{pmatrix} \quad (10)$$

Further, $Ec = \frac{\mu C_p}{k}$, $\text{Pr} = \frac{U^2}{C_p T_w}$, represent Eckert number, Prandtl number, also

$$A_1 = \left((1-\phi) + \phi \frac{\rho_s}{\rho_f} \right)$$

$$A_2 = (1-\phi) + \phi \frac{(\rho C_p)_s}{(\rho C_p)_f}$$

$$A_3 = \frac{k_{nf}}{k_f} = \frac{k_s + 2k_f - 2\phi(k_f - k_s)}{k_s + 2k_f + \phi(k_f - k_s)}$$

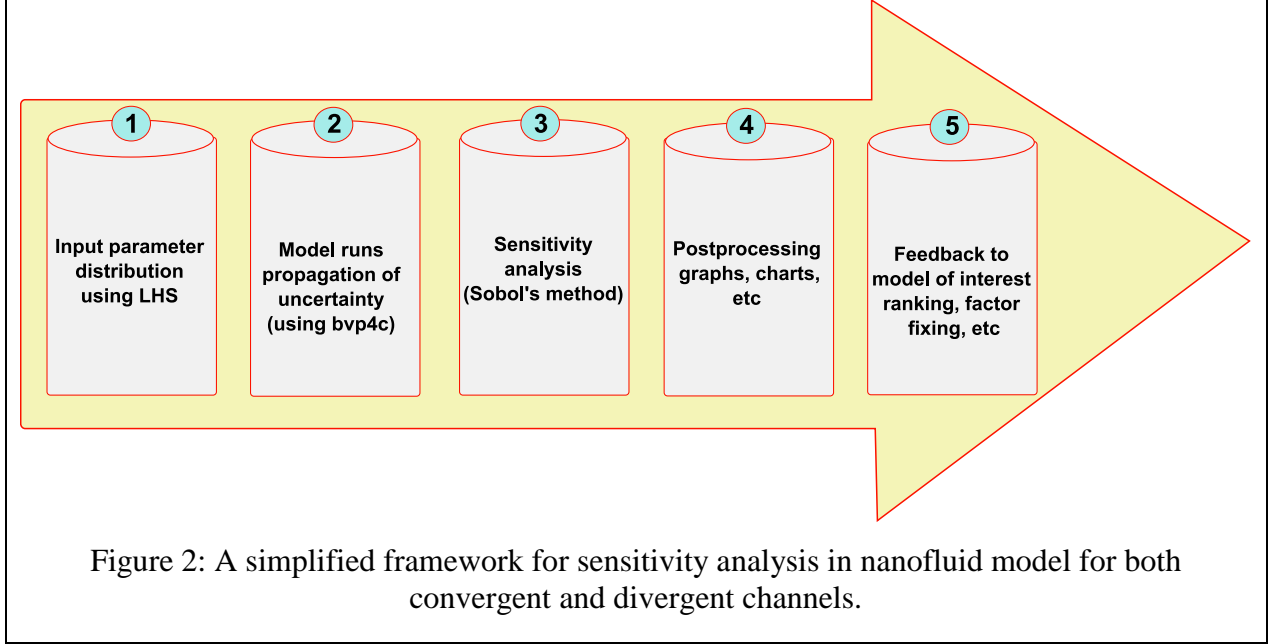
In above equations, primes represent derivative w.r.t. η . Further, $F(\eta)$ and $\beta(\eta)$ are the dimensionless velocity and the temperature profiles, respectively.

Table 1: Thermo-physical properties of base fluid (water) and nanoparticles of copper [13].

	$\rho \left(\frac{\text{kg}}{\text{m}^3} \right)$	$C_p \left(\frac{\text{J}}{\text{kg.K}} \right)$	$k \left(\frac{\text{W}}{\text{m.K}} \right)$
Water (pure)	997.1	4,179	0.613
Copper (Cu)	8,933	385	401

3. The Sobol's method

The method of Sobol is a global sensitivity analysis method in which the output uncertainty caused by input parameters is decomposed and assigned to model input parameters. Due to this reason the Sobol's method is also known as variance-decomposition method. A general procedure to implement the Sobol's method is given in Figure (2). Consider a model of the form $Y = f(X) = f(x_1, x_2, \dots, x_k)$, where, x_1, x_2, \dots, x_k are K uncertain parameters generated independently within a unit hypercube i.e. $x_i \in [0,1]^K$ for $i = 1, 2, 3, \dots, K$



Further, the output uncertainty, Y can be decomposed as [18]:

$$f(x_1, x_2, \dots, x_K) = f_0 + \sum_i^K f_i(x_i) + \sum_i^K \sum_{i < j} f_{ij}(x_i, x_j) + \dots + f_{1,2,\dots,K}(x_1, x_2, \dots, x_K) \quad (11)$$

In Eq. (11), f is integrable, f_0 is a constant, f_i is a function of x_i , f_{ij} is a function of x_i and x_j , and so on, which in terms conditional expected values can be expressed as,

$$\begin{aligned} f_0 &= E(Y) \\ f_i(x_i) &= E_{x \sim i}(Y | x_i) - f_0 \\ f_{ij}(x_i, x_j) &= E_{x \sim ij}(Y | x_i, x_j) - f_0 - f_i - f_j \end{aligned} \quad (12)$$

Where, E denotes expectation value and $x \sim i$ means all parameters other than x_i . The expression for the total variance is,

$$V = \int_{\Omega} f^2(X) dX - f_0^2, \quad (13)$$

Eq. (13) in terms of Eq. (11) is

$$V = \sum_i^K V_i(x_i) + \sum_i^K \sum_{i < j} [V_{ij}(x_i, x_j) + \dots + V_{1,2,\dots,K}(x_1, x_2, \dots, x_K)] \quad (14)$$

Where,

$$\begin{aligned} V_i &= V_{x_i}(E_{x \sim i}(Y | x_i)) = V(f_i(x_i)) \\ V_{ij} &= V_{x_i x_j}(E_{x \sim ij}(Y | x_i, x_j)) - V_i - V_j = V(f_{ij}(x_i, x_j)) \end{aligned} \quad (15)$$

Eq. (14), when divided by V gives,

$$1 = \sum_i^K S_i(x_i) + \sum_{i < j}^K S_{ij}(x_i, x_j) + \dots + S_{1,2,\dots,K}(x_1, x_2, \dots, x_K) \quad (16)$$

where,

$$S_i = \frac{V_i}{V} \quad (17)$$

$$S_{ij} = \frac{V_{ij}}{V} \quad (18)$$

Where, S_i (main effect) stands for impact of i^{th} parameters and S_{ij} represents the mutual impact of i^{th} and j^{th} parameters on output uncertainty. The total effects S_{T_i} or interaction effects of all involved parameters can be computed as,

$$S_{\tau_i} = \frac{E_{x \sim i}(V_{x_i}(Y | x \sim_i))}{V} = 1 - \frac{V_{x \sim i}(E(Y | x \sim_i))}{V} \quad (19)$$

In general, main effects are used to identify the key model parameters and total sensitivity indices (mutual effects of parameters) are used for factor fixing, see Algorithm 1.

Algorithm 1: Algorithm to calculate main effects (S_i) of all involved parameters
<p>1 Input quantities of interest (QoI) := Input model parameters i.e. $\alpha^+, \alpha^-, \text{Re}, \phi$, and Ec. Output quantities of interest (QoI) := Velocity profile and temperature distribution.</p> <p>2: Generate two random numbers matrices, A and B of order $N \times K$ using LHS. Where, N and K are the total count of model simulations and uncertain parameters respectively.</p> <p>3: for $i = 1:N$ Solve the model for different parameter sets given in matrices A and B and save as Y_A and Y_B respectively. end of i loop.</p> <p>4: for $j = 1:K$, generate another matrix C_j, which is identically equal to the matrix A other than the j^{th} column taken from matrix B. Again, model simulations for each C_j are saved as Y_{C_j}.</p> <p>5: for $p = 1:T_s$, where T_s := output time series = 2, for $t = 1:t_p$, where t_p := total no. of time points between 0 and 1, compute and save the sensitivity time series, S_t for both velocity profile</p>

and temperature distribution w.r.t. each parameter at each time point using Jansen operator (estimator) [28,29].

$$S_t = 1 - \frac{1}{2NV} \sum_{n=1}^N (Y_B^n - Y_C^n)^2,$$

where,

$$V = \frac{1}{N} \sum_{n=1}^N (Y_B^{(n)})^2 - E^2, \text{ and } E = \left(\frac{1}{N} \sum_{n=1}^N (Y_B^{(n)})^2 \right).$$

end of t, p and j loops

6: for s = 1: K, compute S_i .

end of s loop.

4. Convergence of sensitivity indices

In this work, we used Latin hypercube sampling which covered the parameter spaces completely as compared to simple random sampling, see Figure (3). In order to compute main, S_i and total effects, S_{T_i} the method of Sobol needs $N(K + 2)$ model runs. Like, if $N = 10000$ then the total model runs requires to compute both S_i and S_{T_i} , are: $N(+2) = 10000(4 + 2) = 60000$. Initially, sensitivity indices are computed for $N = [1000, 2000, 3000, 5000, 7000, 10000]$ model runs, where the convergence is achieved when N is around 3000.

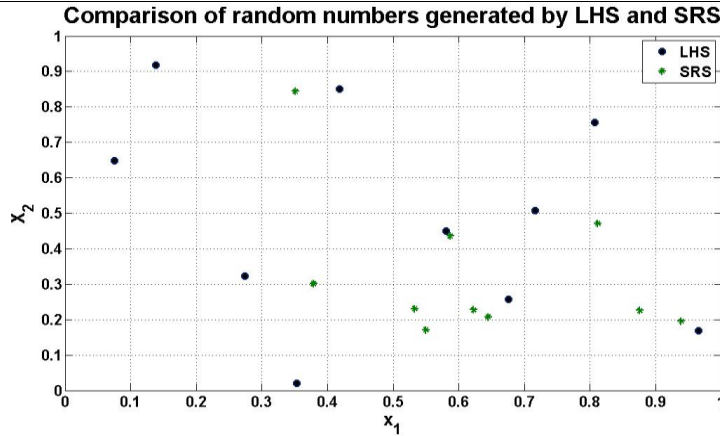
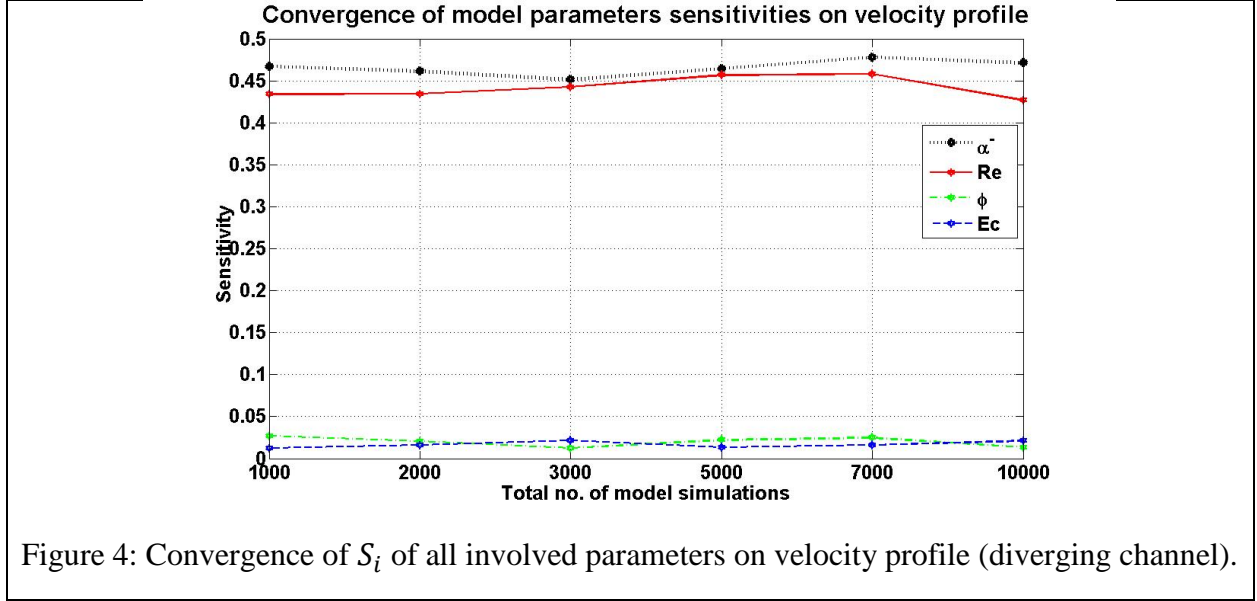


Figure 3: A comparison between Latin hypercube sampling (LHS) and simple random sampling (SRS).

Figure (4) highlights the convergence of model parameters sensitivities on velocity profile for

diverging channel case. It can be observed that with increasing number of simulations, the values for each parameter converge. Same is the case with the temperature distribution for diverging channel (Figure 5). Further, we have used the central limit theorem to calculate the convergence of parameters sensitivities for each output QoI that lies within $\pm 5\%$ of output uncertainty; which is around 3000 model runs.



Similarly, the convergence of model parameters sensitivities for converging channel for both velocity profile and temperature distribution is highlighted in Figures (6) and (7), respectively. Clearly, we can see that with the higher number of simulations, the model parameters converge to a single value and 3000 simulations are enough to attain the convergence.

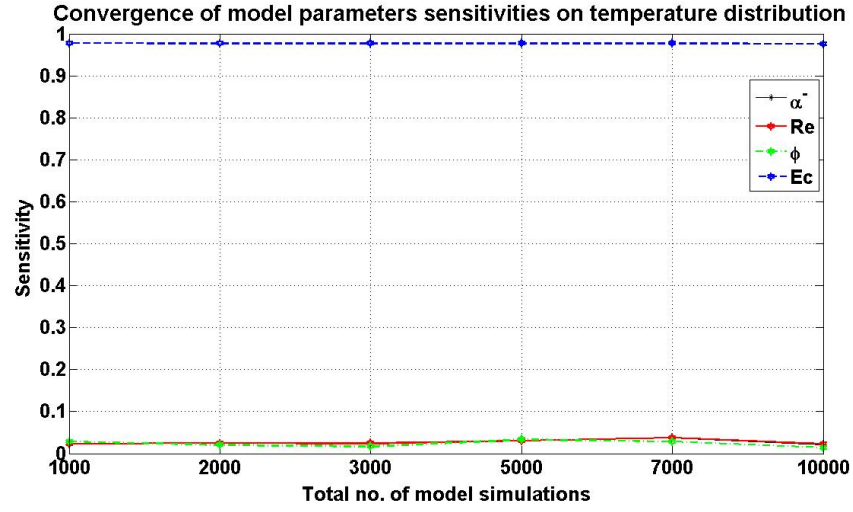


Figure 5: Convergence of S_i of all involved parameters on temperature distribution (diverging channel).

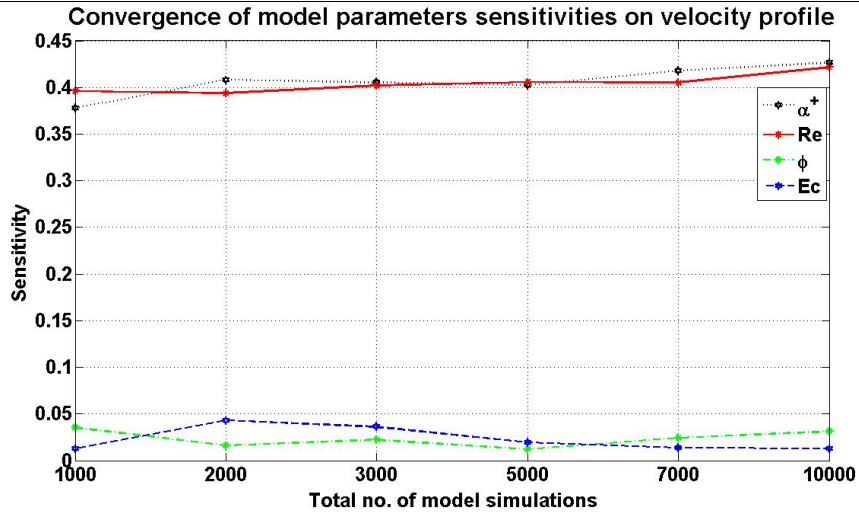


Figure 6 Convergence of S_i of all involved parameters on velocity profile (converging channel).

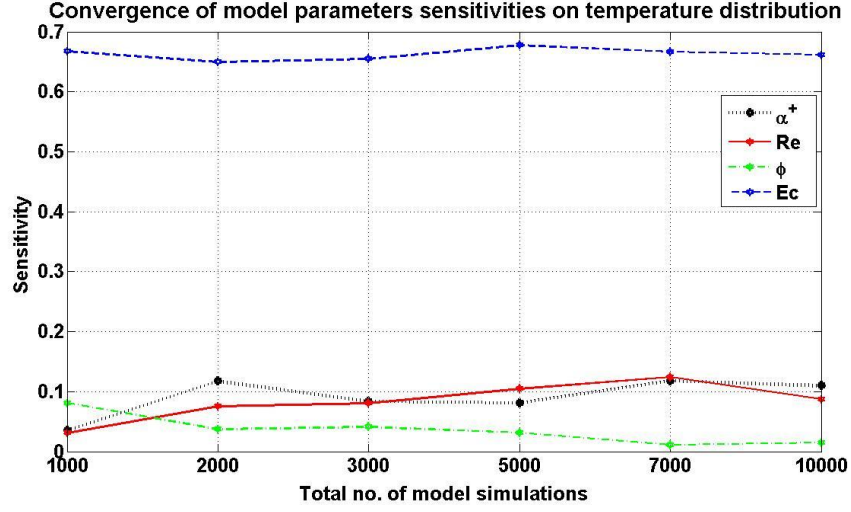


Figure 7: Convergence of S_i of all involved parameters on temperature distribution (diverging channel).

6. Solution procedure and its computational cost

To run model simulation for sensitivity analysis, a MATLAB built in solver bvp4c is used [28-29]. The time taken for one model run is 13s which is suitable for conducting uncertainty and sensitivity analysis. The total time to compute sensitivity indices for all parameters with $N = [1000, 2000, 3000, 5000, 7000, 10000]$ is 10 hours. For model simulations, we used a laptop (Intel (R) CORE i5, 8 GB of RAM). Table (2) gives a detailed description of number of simulations and the time consumed.

Table 2: Computational cost for the simulations

Number of simulations	Time consumed (in seconds)
1000	1763.06
2000	2772.00
3000	4152.50
5000	7618.90
7000	10277.60
10000	14797.90

7. Results and discussions

This section is dedicated to analyze the results obtained for different output QoI. For the said purpose, Figures (8-17) are plotted. Figure (8) gives a description of simulations for the velocity profile in diverging channel. It is evident that the major impact of α on velocity profile is at the lower part of the channel and near the walls velocity profile is almost undisturbed. For the case of temperature distribution, however the main impact is in the middle part as well as near the walls of the channel (Figure 9).

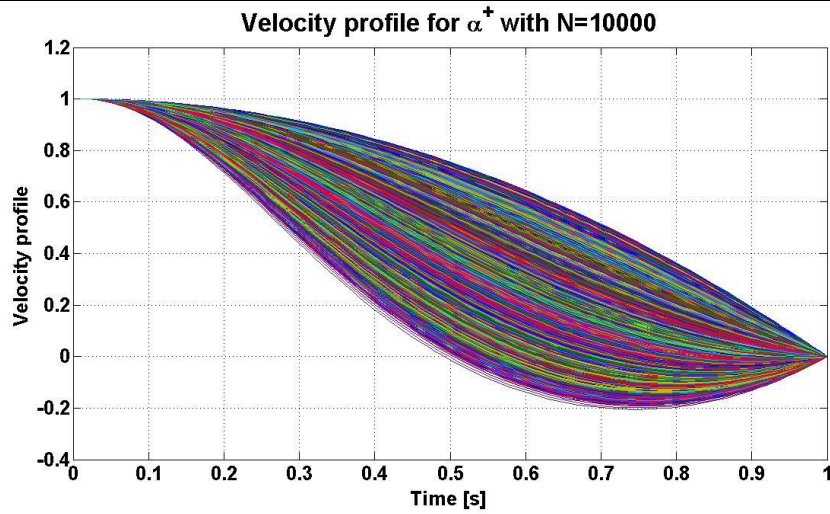


Figure 8: Simulations for velocity profile (diverging channel).

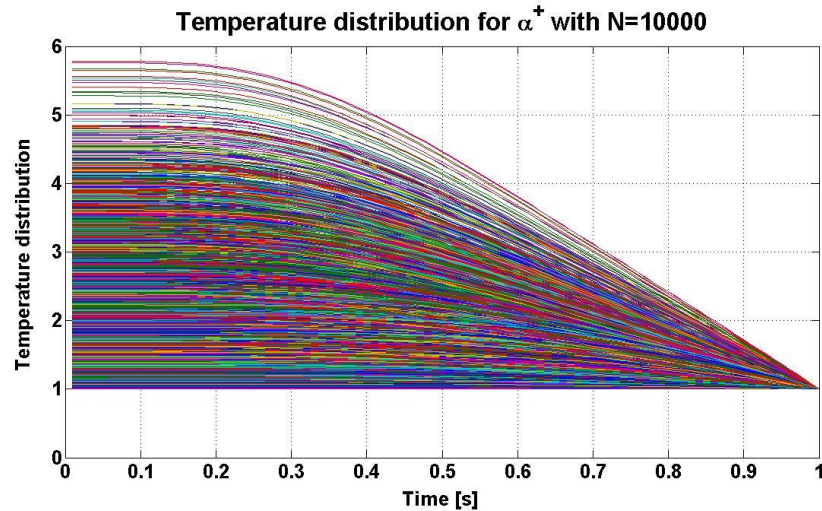


Figure 9: Simulations for temperature distribution (diverging channel).

For the converging channel case, again major impact of α is at the upper part of the channel as well as near the walls velocity is not disturbed much as it is clear from the Figure (10). However, for temperature distribution, most of the sensitivities lies at the middle of the channel without effecting the temperature near the walls of channel (Figure 11).

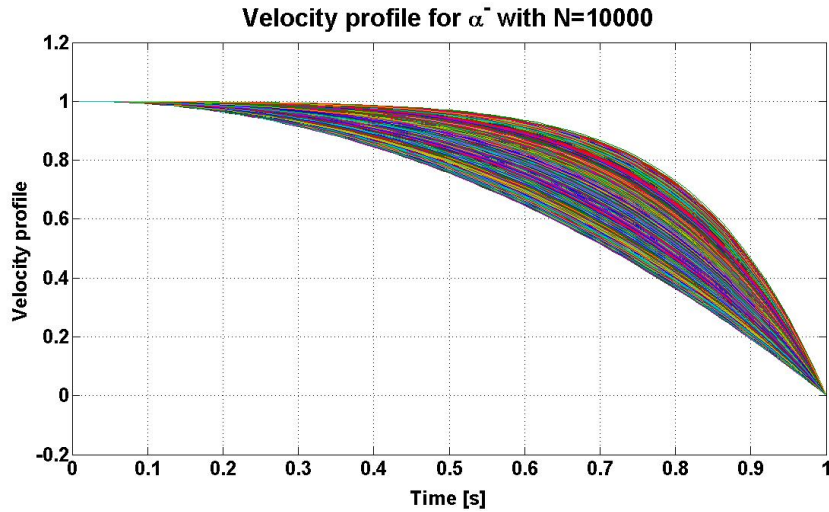


Figure 10: Simulations for velocity profile (converging channel).

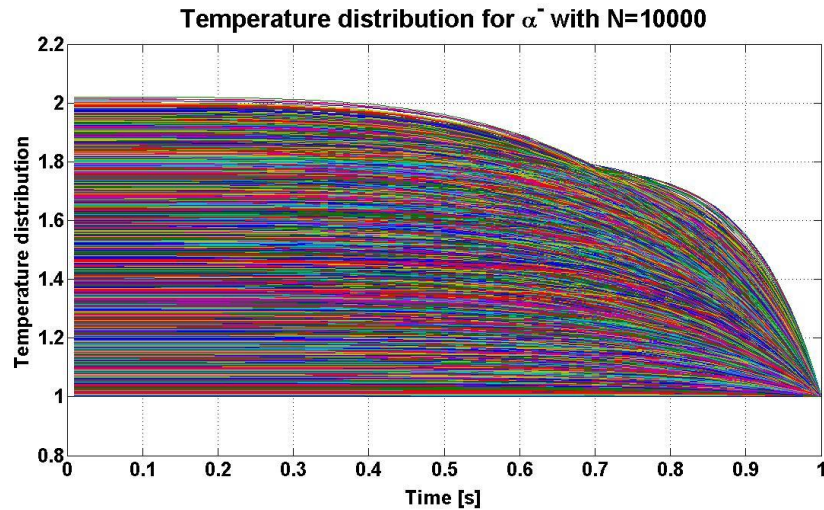


Figure 11: Simulations for temperature distribution (converging channel).

Figure (12) gives a detailed description of sensitivity of involved input parameters (QoI) for the diverging channel. For the velocity distribution, two parameters α (47.23%) and the Reynolds

number (Re) (42.66%) have the major impact. The most sensitive of these parameters is the angle opening α . Furthermore, the other two parameters, the volume fraction of nanoparticles and the Eckert number have almost no effect on the velocity profile for diverging channel. Also, we can identify here that the α and Re may act as bifurcation parameters. For the case of temperature distribution, the most influential parameter is the Eckert number (Ec) (97.63%). Further, the impact of other three parameters is almost negligible.

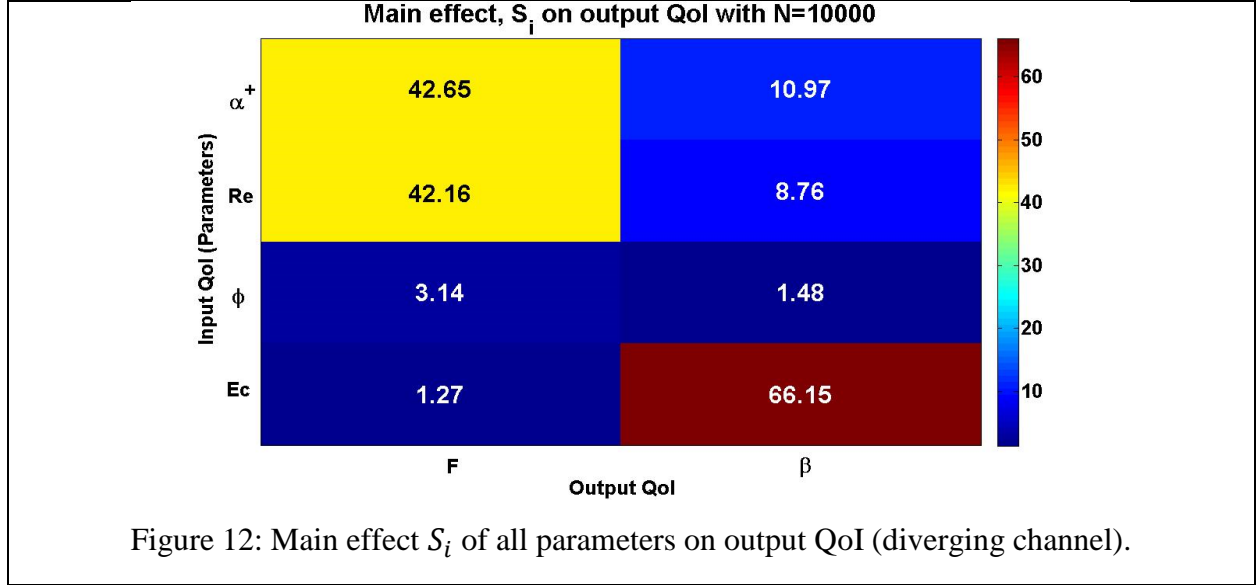
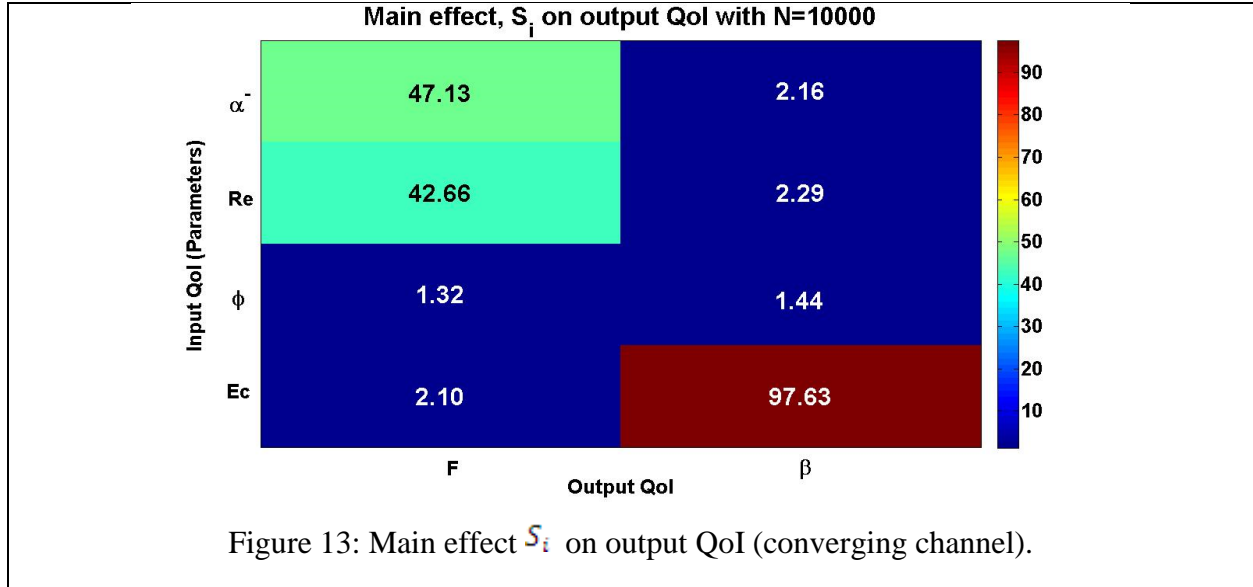


Figure (13) highlights the sensitivity of various parameters for converging channel case. In this case, there is a slight variation in sensitivity of model parameters. The channel opening α and the Reynolds number (Re) have almost the same values, i.e. 42.65% and 42.16%. Both these parameters may act as bifurcation parameters for converging channel case. For the temperature distribution, again there is a change in sensitivities of model parameters for converging channel. The Eckert number (Ec) is the most influential parameter (66.15%) followed by the channel opening α (10.97%) and the Reynolds number (Re) (8.76%). It is also pertinent to mention that each column of Figures (12) and (13) represent the ranking of influential parameters. For example in Figure (13), for velocity profile, α (47.13%) is the most influential parameter followed by Reynolds number (42.66%), the Eckert number (2.10%) and volume fraction of nanoparticles (1.32%).



The upcoming Figures highlights the interaction effects of input QoI on velocity and the temperature profiles. Figure (14) shows these effects for the case of diverging channel. One can easily observe that the channel opening α has a 13.83% interaction effect when compared to all the other parameter. Similarly, the Reynolds number Re has 12.28% interaction effects when combined with all other parameters or input QoI. Next comes the nanoparticle volume fraction ϕ with 0.53% followed by Eckert number with 0.30%. For temperature profile, Reynolds number have the highest interaction effects (11.85%) followed by the channel opening α (9.97%), Eckert number (7.09%) and nanoparticle volume fraction (0.29%).

In Figure (15), interaction effects of input QoI for the converging channel case are presented. Here, Reynolds number becomes the most dominating factor with 10.46% interaction effects when combined with the other involved parameters. Then comes α with 8.78% followed by Eckert number (1.17%) and the nanoparticle volume fraction ϕ (1.01%). For the temperature profile, ϕ becomes the most dominating parameter with the interaction effects of 1.34%. Reynolds number comes next with 1.02% interaction effects followed by Eckert number (0.96%) and the channel opening α (0.93%).

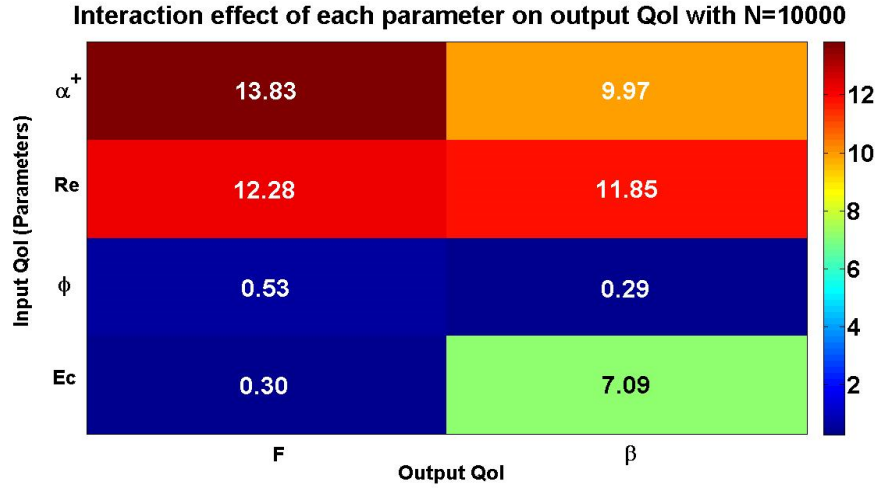


Figure 14: Mutual (interaction) effects of all involved parameters on outputs for diverging channel.

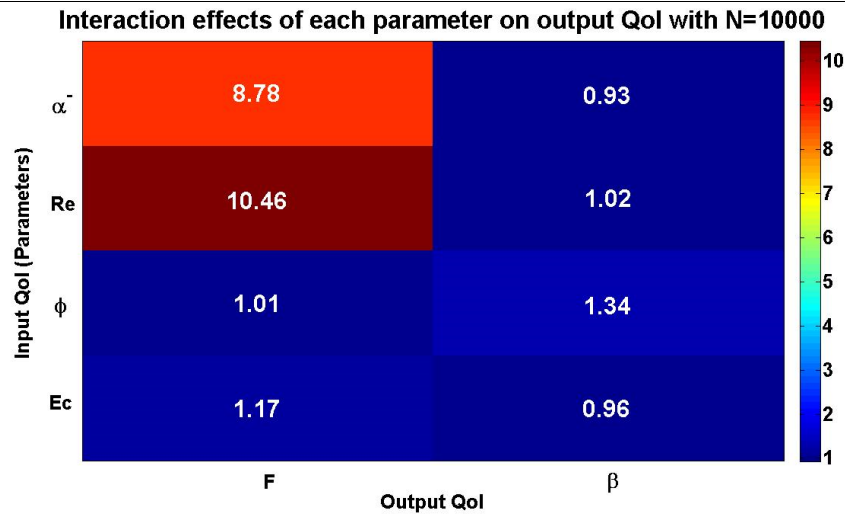


Figure 15: Mutual (interaction) effects of all involved parameters on outputs for converging channel.

8. Conclusions:

Sensitivity analysis for the flow of nanofluids in converging and diverging channels is presented.

Base on our analysis the following important conclusions can be drawn:

- For the velocity profile, α is the most inflential parameter for velocity profile. While, for temperature distribution, Ec is the most influential parameter.
- On the basis of our analysis, for the diverging channel, α is the key parameter followed

by Re , ϕ and Ec in the case of velocity profile. When it comes to temperature profile, Ec becomes the most important parameter, followed by α , Re and ϕ respectively.

- In the case of converging channel, α is the most sensitive parameter for velocity profile followed by Re , Ec and ϕ respectively. For temperature distribution, Ec number is the most influential parameter followed by Re , α and ϕ respectively.

References

- [1]. S. S. Choi, J.A. Eastman, Enhancing thermal conductivity of fluids with nanoparticle, in: D.A. Siginer, H.P. Wang (Eds.), *Developments and Applications of Non-Newtonian*, vol. 66 (1995) 99-105.
- [2]. J. Buongiorno, Convective transport in nanofluids, *ASME Journal of Heat Transfer*, 128 (2006) 240-250.
- [3]. Q. Xue, Model for thermal conductivity of carbon nanotube-based composites, *Physica B: Condensed Matter*, 368 (2005) 302-307.
- [4]. S. M. Murshed, C. Sohel, N. D. Castro, M. Lourenço, M. Lopes, F. Santos, A review of boiling and convective heat transfer with nanofluids, *Renewable and Sustainable Energy Reviews*, 15(5) (2011) 2342-2354.
- [5]. W. Khan, I. Pop, Boundary-layer flow of a nanofluid past a stretching sheet, *International Journal of Heat and Mass Transfer*, 53 (2010) 2477–2483.
- [6]. A. Kuznetsov, D. Nield, The Cheng–Minkowycz problem for natural convective boundary-layer flow in a porous medium saturated by nanofluid, *International Journal of Heat and Mass Transfer*, 52 (2009) 5792-5795.
- [7]. M. Sheikholeslami, D. Ganji, M. Javed, R. Ellahi, Effect of thermal radiation on magnetohydrodynamics nanofluid flow and heat transfer by means of two-phase model, *Journal of Magnetism and Magnetic Materials*, 374 (2015) 36-43.
- [8]. N. Ahmed, S. T. Mohyud-Din, S. M. Hassan, Flow and heat transfer of nanofluid in an asymmetric channel with expanding and contracting walls suspended by carbon nanotubes: A numerical investigation, *Aerospace Science and Technology*, 48 (2016) 53-60.
- [9]. W.A. Khan, I. Pop, Boundary layer flow past a wedge moving in a nanofluid. *Mathematical Problems in Engineering*, Volume 2013, Article ID 637285.

- [10]. U. Khan, N. Ahmed, S. T. Mohyud-Din, B. Bin-Mohsin, Nonlinear radiation effects on MHD flow of nanofluid over a nonlinearly stretching/shrinking wedge, *Neural Computing and Applications*, 28 (8) (2017) 2041–2050.
- [11]. G.B. Jeffery, The two-dimensional steady motion of a viscous fluid, *Philosophical Magazine and Journal of Science*, 6 (1915) 455–465.
- [12]. G. Hamel, Spiralförmige Bewegungen Zäher Flüssigkeiten, *Jahresber. Deutsch Math Verein*, 25 (1916) 34–60.
- [13]. S. T. Mohyud-Din, U. Khan, S. M. Hassan, Numerical investigation of magnetohydrodynamic flow and heat transfer of copper–water nanofluid in a channel with non-parallel walls considering different shapes of nanoparticles, *Advances in Mechanical Engineering*, 8 (3) (2016) 1-9.
- [14]. U. Khan, N. Ahmed, S.T. Mohyud-Din, Heat transfer effects on carbon nanotubes suspended nanofluid flow in a channel with non-parallel walls under the effect of velocity slip boundary condition: a numerical study, *Neural Computing and Applications*, 28 (2017) 37–46.
- [15]. S. T. Mohyud-Din, U. Khan, N. Ahmed, S. M. Hassan, Magnetohydrodynamic Flow and Heat Transfer of Nanofluids in Stretchable Convergent/Divergent Channels, 5(4) (2015) 1639-1664.
- [16]. R. Gul, Mathematical modeling and sensitivity analysis of lumped-parameter model of the human cardiovascular system. PhD Thesis, FU Berlin, Germany (2016).
- [17]. Z. Zi, Sensitivity analysis approaches applied to systems biology models. *IET system biology*, 5 (6) (2011) 336-346.
- [18]. R. Gul, S. Bernhard, Parametric uncertainty and global sensitivity analysis in a model of the carotid bifurcation: Identification and ranking of most sensitive model parameters. *Mathematical Biosciences*, 269 (2015) 104-116.
- [19]. A. Saltelli, M. Ratto, T. Andres, F. Campolongo, J. Cariboni, D. Gatelli, M. Saisana, S. Tarantola, *Global Sensitivity Analysis. The Primer*, John Wiley Sons (2008).
- [20]. A. Saltelli, A., S. Tarantola, K.P.S. Chan, A quantitative model-independent method for global sensitivity analysis of model output. *Technometrics*, 41(1) (1996) 3956.
- [21]. M.D. Morris, Factorial sampling plans for preliminary computational experiments. *Technometrics*, 33, 161174 (1991).

- [22]. I. Sobol, Sensitivity estimates for nonlinear mathematical models. *Matematicheskoe Modelirovanie* 2, 112118. In Russian, translated in English (1990).
- [23]. T. Homma, A. Saltelli, Importance measures in global sensitivity analysis of nonlinear models. *Reliability Engineering and System Safety*, 52 (1996) 117.
- [24]. P. Chen, A. Quarteroni, G. Rozza, Simulation-based uncertainty quantification of human arterial network hemodynamics. *International Journal for Numerical Methods in Biomedical Engineering* 00, 1-24 (2013).
- [25]. Darbari B, Rashidi S, Abolfazli Esfahani J. Sensitivity analysis of entropy generation in nanofluid flow inside a channel by response surface methodology. *Entropy*. 2016 Feb;18(2):52.
- [26]. Mackolil J, Mahanthesh B. Sensitivity analysis of radiative heat transfer in Casson and nano fluids under diffusion-thermo and heat absorption effects. *The European Physical Journal Plus*. 2019 Dec 1;134(12):619.
- [27]. Fadodun OG, Amosun AA, Okoli NL, Olaloye DO, Durodola SS, Ogundeji JA. Sensitivity analysis of entropy production in Al_2O_3/H_2O nanofluid through converging pipe. *Journal of Thermal Analysis and Calorimetry*. 2019:1-4.
- [28]. M.J. W. Jansen, Analysis of variance designs for model output. *Computer Physics Communications*, 117 (1999) 35-43.
- [29]. M.J. W. Jansen, W.A.H. Rossing, R.A. Daamen, Monte Carlo estimation of uncertainty contributions from several independent multivariate sources. *Predictability and Nonlinear Modeling in Natural Sciences and Economics*, Kluwer Academic Publishers, Dordrecht, 334-343 (1994).